Chapter 5

Microwave and THz Metamaterial-Based Devices for Potential Applications in NDE, Chem-Bio Detection and Dielectric Characterization of Complex Oxide Thin Films

Daniel Shreiber

Additional information is available at the end of the chapter

http://dx.doi.org/10.5772/65951

Abstract

The purpose of this chapter is to convey a message that the variety of applications of the classical (and the novel ones, such as Mie resonance based) metamaterials are going far beyond the originally proposed applications such as geometrical optics and antennas. In addition, it is important to mention that most of these applications are just an idea or a first proof of principle. Hence, an additional message of this chapter is that a lot of further research is required to implement these scientifically sound ideas. It is also a hope that this chapter will trigger the reader's curiosity and interest to pursue this exciting field, which will yield additional applications that have never been imagined.

Keywords: MW and THz metamaterials, NDE, chem/bio detection, dielectric properties characterization, complex oxide thin films

1. Introduction

Multiple applications of a new range of materials called metamaterials have been developed since their evolution, suggested by Veselago [1], to the development of their design, first proposed by Pendry et al. [2, 3]. Most notably, the proposed applications included antennas [4] and geometrical optics [5]. Indeed, the proposed metamaterial-based structures were designed to enhance the antenna properties such as bandwidth, or geometrical optics properties such as reduced aberrations and enhanced focusing by the metamaterial lens [6].

In the years to follow, extensive research in the field of metamaterials yielded novel metamaterial classes (metamaterials based on dielectric resonators, for example) [7] and configurations [8] in addition to the "classical" ones in the form of metallic split ring and a wire designed by Shelby et al. [5] that are shown in (**Figure 1**).

In their original definition, the metamaterials are artificial materials that respond to impinging electromagnetic waves by exhibiting negative values of the permittivity (ε) and/or the permeability (μ). Typically, the metamaterials are divided into double-negative when both values of ε and μ are negative or single-negative when one of these values is negative.

In this chapter, we discuss utilization of the "classical" and other metamaterial devices for a number of applications that go beyond the antenna and geometrical optics application. This approach will demonstrate the extent to which the field of metamaterial applications has grown in recent years, taking this exciting discovery one step further to implementation in real-life devices. Both single-negative and double-negative metamaterial devices are discussed in this chapter. Most of the ideas that are to be discussed here are on the level of proof-of-concept and some of them have a good chance to become real life application in the nearest future.

It is our desire to discuss these concepts in the context of their applications. Hence, it is prudent to provide the background for the application in order to give a complete picture of the concrete capability gaps and how the proposed metamaterial devices can address these shortcomings.

When the "classical" metamaterials are discussed, we refer to each metallized-structure unit cell as to an artificial atom that "reacts" to impinging electromagnetic wave. The dimensions of these structures and their features will determine the resonant frequency of the device.

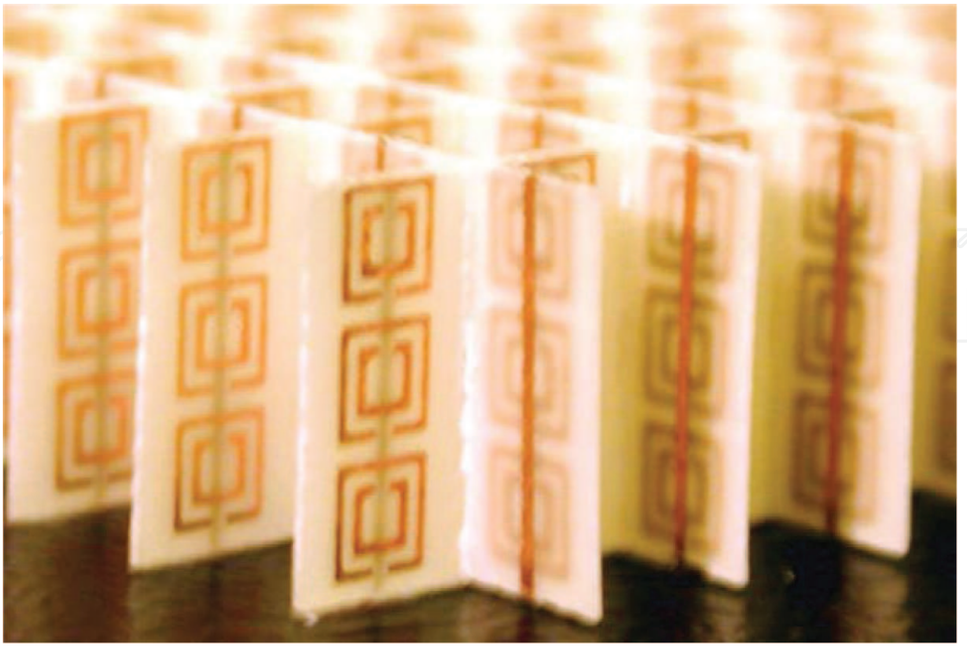

Figure 1. Optical image of a classical metamaterial structure that operates at a resonant frequency of 10.5 GHz[8] (Reproduced with permission of American Association for the Advancement of Science via Copyright Clearance Center).

http://dx.doi.org/10.5772/65951

Typically, such a unit cell measures to about 1/10 to 1/20 of a resonant wavelength and consists of a wire and a split ring (either together for double-negative or one of the two for single-negative). An example of a two-dimensional (2D) double-negative and one-dimensional (1D) metamaterial model and transmission results obtained from the operation of the metamaterial fabricated based on this model [9] are shown in **Figure 2**.

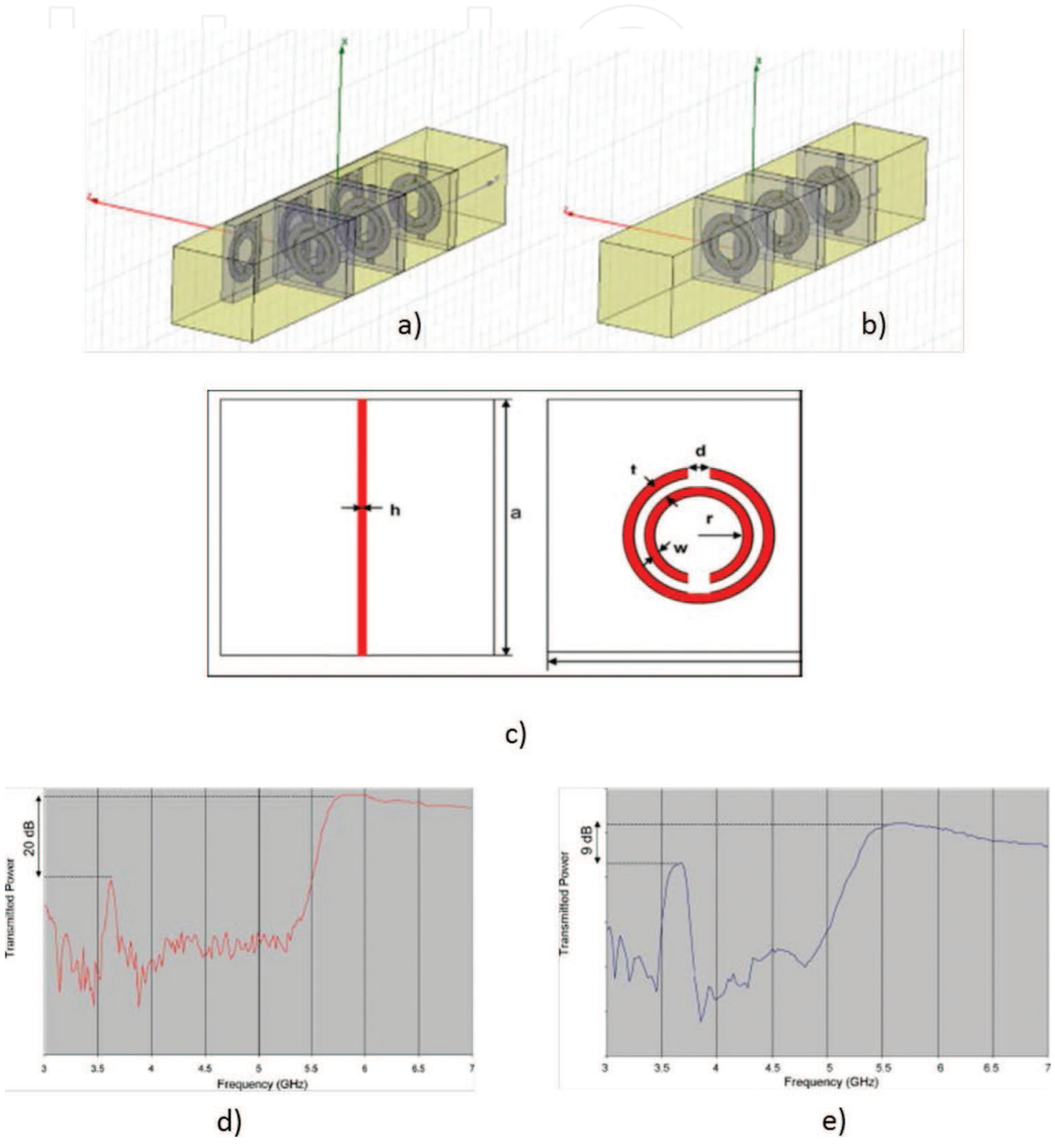

Figure 2. A few unit cells modeled in HFSS Ansoft © for (a) 2D metamaterial and (b) 1D metamaterial slab, (c) dimensions of the metallized components of the designed unit cell are as follows: FR4 (ε = 4.4, tan δ = 0.02), metallic structures—copper (30 μm thick), r = 1.6 mm, $d = t$ = 0.2 mm, w = 0.9 mm, a = 9.3 mm, h = 0.9 mm. PCB sheets were 1.8 mm thick, (d) transmission scan from the structure depicted in (a) and e) transmission scan of a structure depicted in (b) [9]. (Reproduced with permission of ELSEVIER S.A. via Copyright Clearance Center).

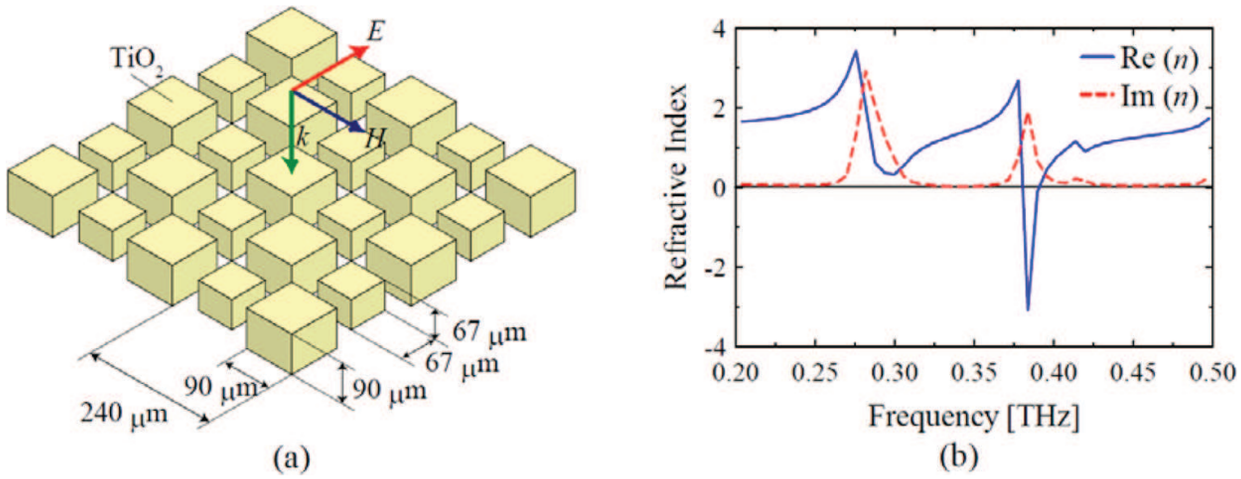

Figure 3. (a) Designed metamaterial structure in the low THz regime, (b) transmission scan showing negative index of refraction for this configuration [10] (reprinted with permission from Shibuya, K., K. Takano, N. Matsumoto, H. Miyazaki, K. Izumi, Y. Jimba, and M. Hangyo,"Terahertz metamaterials composed of TiO2 cube arrays". Proceedings of the Second International Congress on Advanced Electromagnetic Materials in Microwaves and Optics - Metamaterials, Pamplona, Spain 2008, Copyright 2008 Metamorphose IV).

From **Figure 2(d)** and **(e)**, one can see that the resonant frequency of this double-negative metamaterial is 3.65 GHz, which corresponds to a wavelength of about 8.2 cm. **Figure 2(c)** indicates that the largest dimension of the designed structure is the size of the unit cell and, hence, the length of the metallic wire which measures 9.3 mm is about 1/10 of the resonant wavelength.

The same rule of thumb can be applied to alternative metamaterial structures such as an array of TiO_2 oxide cubes used as a metamaterial in low THz range of frequencies [10] which have dimensions of about 1/10 of the lowest resonant frequency measured for this metamaterial system. The model and the transmission scan of this metamaterial structure are depicted in **Figure 3**.

Simulations of the metamaterial system can be used to predict the resonant frequency and hence, the operational frequency of a device.

It is important to keep in mind the dimensions of the metamaterial surface for a particular application/frequency. For example, it may be technically challenging (due to their dimensions and configuration) to implement some metamaterial devices for THz and optical applications [11].

In this chapter, we review the examples of metamaterial device applications in microwave (MW) and terahertz (THz) spectra of radiation. We will look into both single-negative and double-negative metamaterial devices, as well as into active and passive devices. This review is not meant to be an exhaustive list of potential metamaterial applications outside of the antenna and geometrical optics, but just a few ideas of how the very novel concept of artificial materials can be applied in a wide variety of ways.

The remainder of the chapter is divided into individual applications where the background for the application, its configuration, advantages, and limitations will be discussed.

http://dx.doi.org/10.5772/65951

2. Novel nondestructive evaluation (NDE) detector based on a metamaterial lens

The first application that we are going to discuss is a novel NDE detector based on a metamaterial lens. The proposed detector is capable of operating in a low GHz range of frequencies.

2.1. Background

There are many instances where it is important to detect a flaw or inclusion that is not visible to human eye as it is covered by a layer of nonconducting material. Detection through conductive surfaces is limited as they will reflect the waves in the radiation ranges that are typically utilized by metamaterial devices (excluding, probably, acoustical [12]). However, some work has been done to investigate carbon-fiber-reinforced structures with microwaves [13]. One of the examples where the application of such a detector could be highly beneficial is a system where a thick layer of thermal insulation covers a metallic surface (you can think of a space shuttle tile covering shuttle skin, for example). The thermally insulating layer is attached by an adhesive and we do not want to remove in order to determine whether the onset of corrosion had occurred underneath the insulating layer. In order to successfully detect this flaw, two conditions need to be satisfied: (a) the resolution of our detector has to be good enough to detect the flaw and (b) the wave that we are using has to be "strong" enough to penetrate the insulating layer to reach the flaw and to reflect back through the layer to the detector. Here we arrived at a contradiction, though longer wavelengths penetrate further, the resolution of the image will be limited by the wavelength, due to the diffraction limit. Indeed, we could defy the diffraction limit if we investigate the same flaw using the near-field detector, but in many cases, this approach is not realistic since the thickness of the insulator might be larger than the distance that will define the true near field. Additionally, it might not be realistic for real-life devices to maintain the tip of the detector so close to the surface of the sample. As an example, Tabib-Azar et al. demonstrated the resolution of 0.4 μm with 1 GHz wavelength but the tip of their detector was maintained at a very small distance away from the surface of the metal [14].

Pendry [6] analytically demonstrated that a metamaterial lens defies the diffraction limit and, in an ideal case, can transmit all the information emitted from the source. This approach can be utilized when an NDE detector is designed based on a metamaterial lens [15]. Realistically, the detector can serve as a "middle ground" between a far-field and a near-field detector where the standoff distance can be manipulated by the distance of the source from the metamaterial lens and the thickness of the lens, as can be seen from **Figure 4** where the focus spot of the resonant frequency will be significantly smaller than predicted by the diffraction limit.

The equation that shows the distance to the image in the case of an ideal metamaterial lens can be written as:

$$d_1 + d_2 = t. \tag{1}$$

Although Eq. (1) represents the case of an ideal lens which is extremely hard to achieve, the equation gives a very good approximation for the design of such a device.

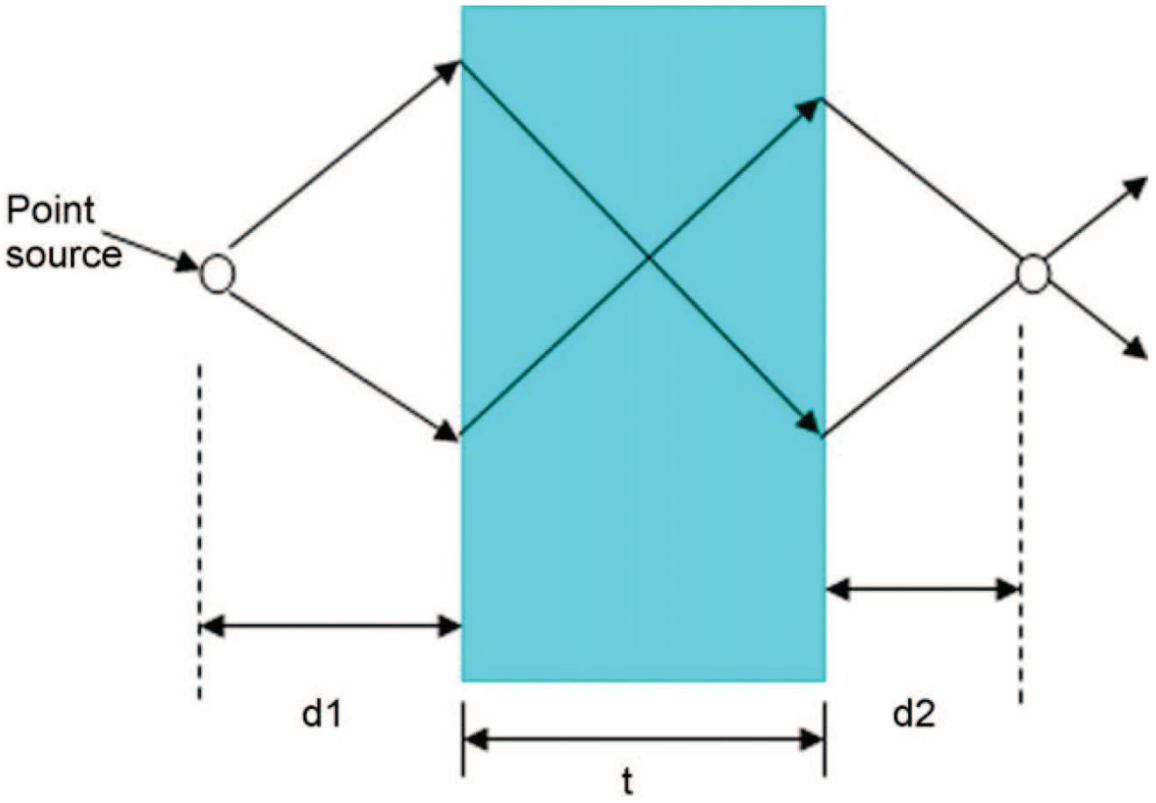

Figure 4. Ray diagram of a metamaterial lens [9] (Reproduced with permission of ELSEVIER S.A. via Copyright Clearance Center).

2.2. Experiment and results

Indeed, the original results are promising. It has been demonstrated [15] that a hole in a fiberglass block with the diameter of 3 mm that is perpendicular to the propagation direction of the electromagnetic wave (**Figures 5** and **6**) can be detected with a device operating at a resonant frequency of 3.65 GHz (8.2 cm). Therefore, the resolution of such a device is determined to be 0.037 λ, which is far below the diffraction limit predictions.

The detection of the location of the hole and of a shift in the hole location are shown in **Figure 6**.

To better understand the effect of the metamaterial lens that was utilized in this proof-of-concept experiment, one can observe that at the frequency of 6 GHz, the location of the holes is not detectable at all as the same lens does not exhibit metamaterial properties, and therefore the electromagnetic wave just passes through the structure and reflects back from the sample into the detector (although the wavelength at this frequency is shorter than at 3.65 GHz). The results of this experiment are shown in **Figure 7**.

It is also important to mention that a lot of thought should be dedicated to the design of the metamaterial lens when considering the inevitable trade-offs. As it was mentioned before, the metamaterial structures are typically very lossy. Therefore, when an NDE detector is designed based on a double-negative metamaterial lens where a high-strength transmitted signal is needed to maintain an adequate signal-to-noise ratio, one should keep in mind the limitations of the system in terms of losses. Sometimes, it is possible to trade off the resolution of the system for better transmission. For example, a 1D structure of parallel (in the direction of the

http://dx.doi.org/10.5772/65951

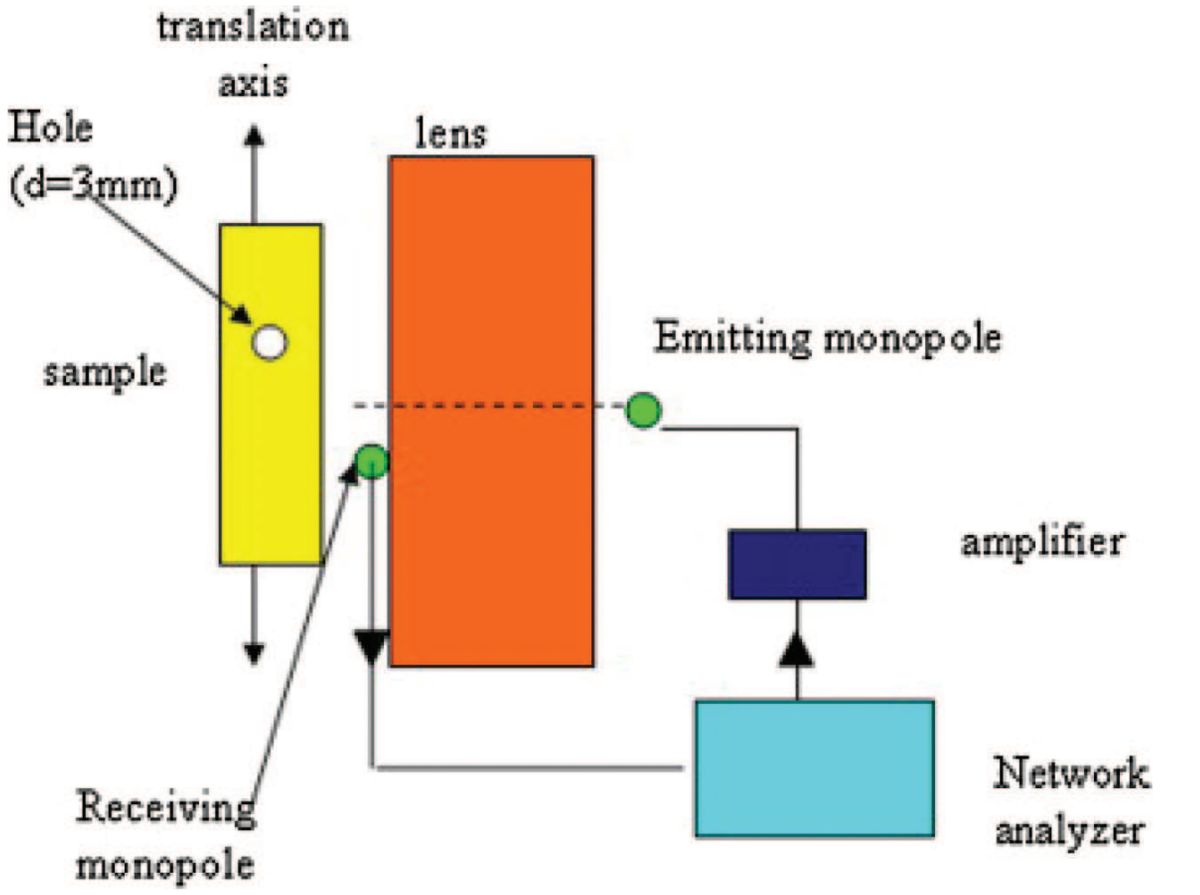

Figure 5. Sketch of the NDE sensor system used to detect the hole defect [15] (Reproduced with permission of ELSEVIER S.A. via Copyright Clearance Center).

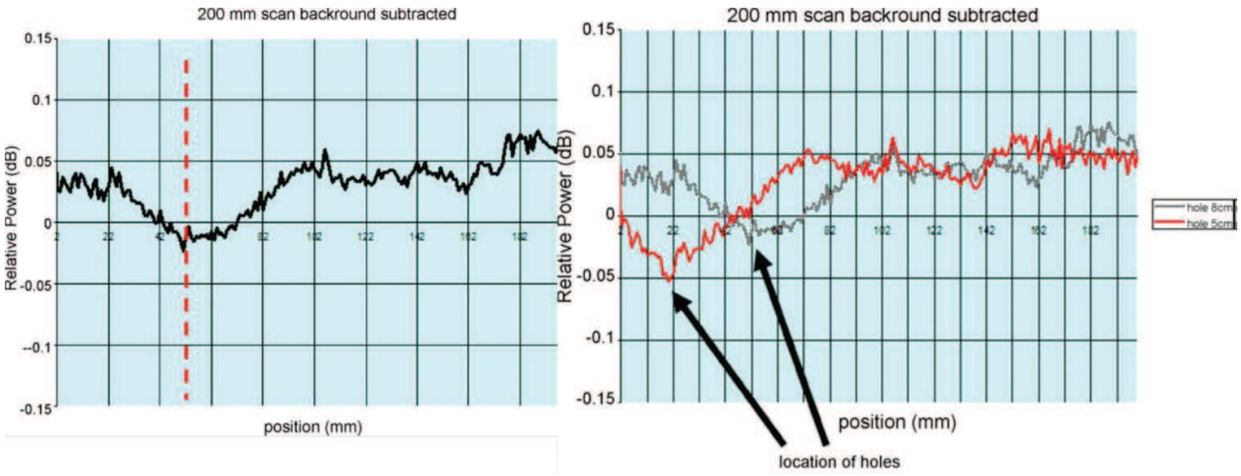

Figure 6. Relative power scan of a sample with one hole and when two holes were sealed with a filler alternately ($f = 3.65$ GHz). The second hole was drilled 3 cm away from the first one [15] (Reproduced with permission of ELSEVIER S.A. via Copyright Clearance Center).

electromagnetic wave propagation) plates with metallized metamaterial unit cells (**Figure 2(b)**) could be used instead of a 2D wine-crate structure for the metamaterial lens. The comparative losses obtained through a power scan are depicted in **Figure 2(d)** and **(e)**. The transmission

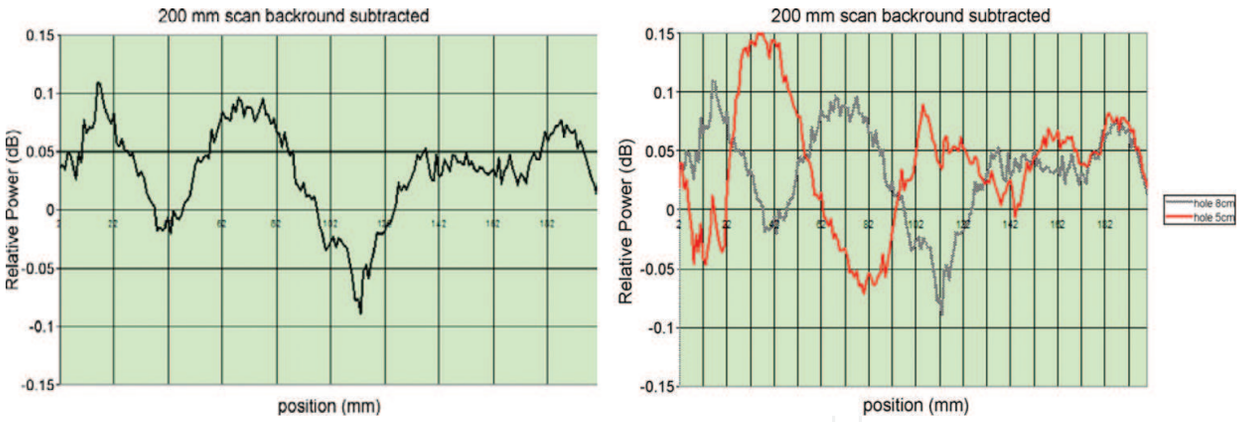

Figure 7. Relative power scan of a sample with a hole and when two holes were filled alternately ($f = 6$ GHz). The second hole was drilled 3 cm away from the first one [15] (Reproduced with permission of ELSEVIER S.A. via Copyright Clearance Center).

peak for a 2D lens is at −20 dB compared to the transmission through the same lens at frequencies where the lens does not exhibit metamaterial properties (at about 6 GHz). In contrast the same peak for a 1D lens is at −9 dB.

Another trade-off to be considered is how much penetration we really need into the sample to successfully perform the nondestructive evaluation versus the required resolution. In other words, maybe, an NDE detector could be designed to work at a higher frequency, hence, it might not penetrate as far into the dielectric, but the resolution of the metamaterial lens operating at the appropriate frequency will be much better. In that case, we need to consider the fabrication limitations of the metamaterial lens since it is possible that the designed operating frequency of our metamaterial device forces the use of more complicated fabrication methods, such as those that are utilized for devices operating in the THz spectrum.

Also, as we previously mentioned, one can consider alternative metamaterial structures such as oxide metamaterials for these applications where the losses are smaller.

In conclusion, utilization of a metamaterial lens as a tool to significantly enhance capabilities of the nondestructive evaluation detectors has been demonstrated to be successful. This initial proof-of-concept can serve as a very solid foundation from which intensive research and development can build upon to bring these detectors to wide acceptance. The main advantage of these detectors would be a significantly higher resolution at the frequencies that can penetrate relatively far into dielectric materials, while maintaining a comfortable standoff distance for the user.

3. Detection of chem/bio hazards with a metamaterial-based device in THz spectrum

One of the important benefits of the recently discovered THz spectrum of radiation is that most large chemical molecules are resonant in this spectrum as shown, for example, in [16]. There is a significant body of work dedicated to the characterization of DNA molecules [17] in the THz spectrum. In fact, it was suggested that these molecules have multiple unique resonant frequencies in the THz spectrum [18]. Hence, it is possible to uniquely identify these chemical

http://dx.doi.org/10.5772/65951

hazards by the combination of these unique resonant frequencies in the THz spectrum. It is also desired to detect these substances in very low concentrations. It was suggested [18] that one approach that exhibits the highest sensitivity is a detector constructed with a single-negative metamaterial surface. This single-negative metamaterial surface, where the metallic split-ring resonators (SRRs) are resonating at the same frequency as the molecule under investigation, could have the effect of overlapping resonances when this molecule "lands" in the gap of the SRR. The overlapping resonance has a nonlinear effect and, hence, could enhance the sensitivity of the method by 10^6–10^7. The original metamaterial structure for this approach is depicted in **Figure 8**.

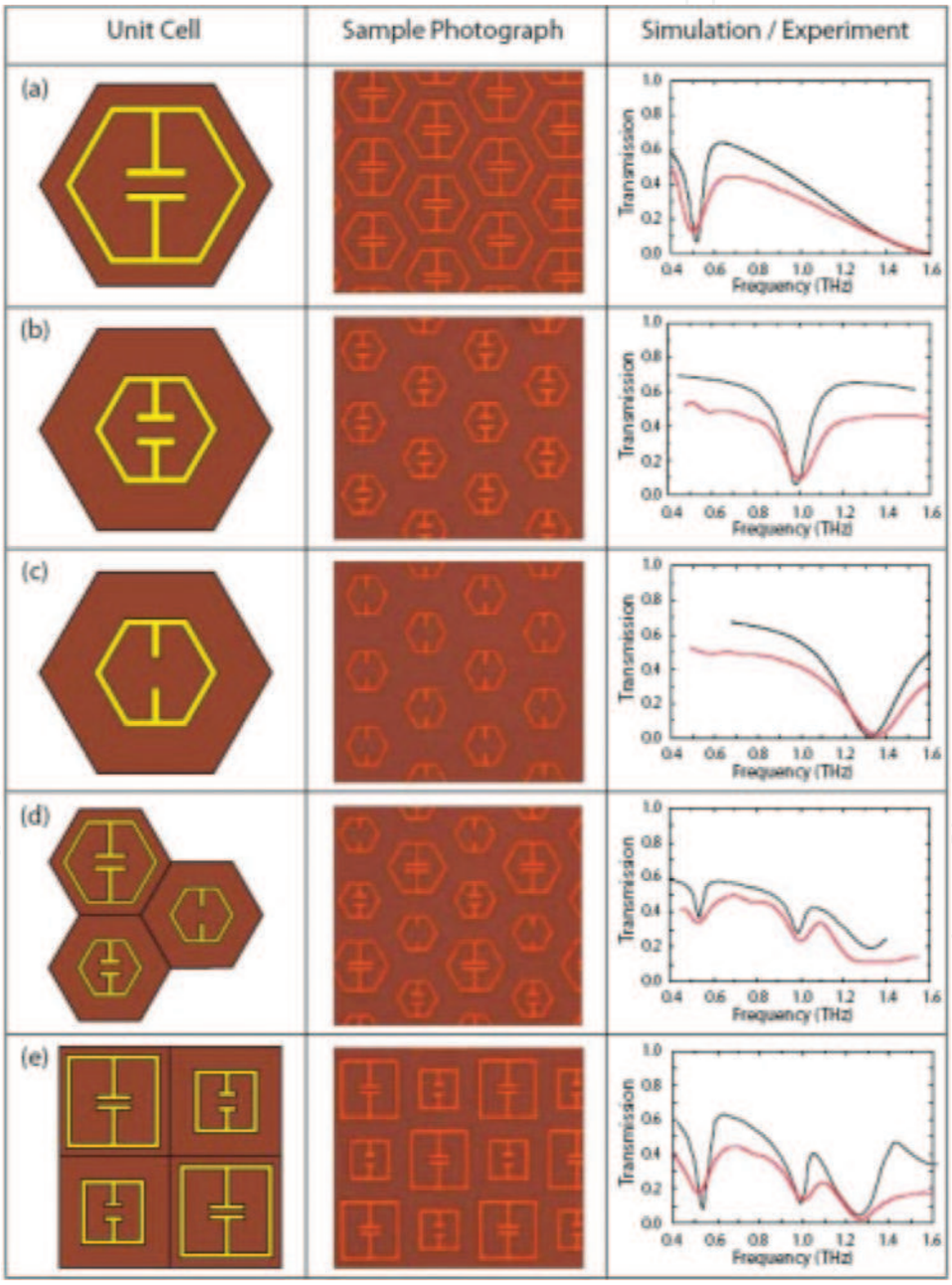

Figure 8. A set of structures designed to act as a metamaterial detector in the THz spectrum for bio substances [18] (Reproduced with permission of OSA).

The simulated and experimental transmission spectra clearly demonstrate a shift in the resonant frequency of the metamaterial device when the design of the metamaterial unit cell is changed. Introduction of a metamaterial surface that contains all three designs will yield multiple resonant peaks.

The issue that the proposed approach faces when a metamaterial structure is designed for real applications is that, as was mentioned before, the classical metamaterial SRRs are resonant in a very narrow band of frequencies. Hence, in order to uniquely detect even one substance (based on the measured values of resonant frequencies) we need to fabricate a device containing a few unique SRR designs.

However, the proposed structure could be optimized if the dielectric properties of the substrate surface (where the SRRs are fabricated on) can be tuned by the application of a simple electrical bias.

It could be suggested that tunable complex oxide thin films can be used to address this challenge. Indeed, the tunability of these films that are typically about 200 nm thick is over 50% [19] when a bias field of about 500 kV/cm is applied. For practical purposes we are restricted to utilize the film of 200 nm or similar thickness as the fields required for the tunability effect are prohibitively high (about 600 kV/cm [20]) and, therefore, thin films are necessary so that practical voltages of about 5–10 V can be used. Fabrication of the tunable complex oxide thin films is not trivial and their dielectric properties are much more challenging to stabilize when compared to bulk materials due to the dependence of these properties (such as dielectric constant, tunability, losses, and leakage current) on factors as coefficient of thermal extension (CTE) mismatch between the substrate and the film yielding a stress that affect the dielectric properties [21]. In addition, proper bias electrodes must be used in such a structure. For example, transparent conductive oxide electrodes such as indium tin oxide (ITO) can be used, however, certain measures have to be taken during the thin film growth to extend the transparency of this material into the THz spectrum from the optical. A typical response (frequency scan) from a single-negative metamaterial is presented in **Figure 9**.

If the resonant frequency of the metamaterial surface could be matched with the resonant frequency of a molecule resulting in the overlapping resonance, we anticipate an even stronger response on the frequency scan at the resonant frequency, which will indicate the presence of a substance under investigation.

Alternative metamaterial structures such as ceramic metamaterials [10] could be considered for the same purpose. Again, the benefit of using these novel structures could be reduced losses and, therefore, a possible "sharper" reaction to the overlapping resonances.

Alternative methods for metamaterial device utilization in the THz spectrum for detection and analysis of chem/bio molecules have been proposed in [22]. Ding et al. suggested the use of asymmetrical split-ring resonators as a unit cell for a single-negative metamaterial surface (**Figure 10**).

This approach produced a metamaterial device that, in a response to an impinging THz wave, yielded simultaneously high Q quadrupole and Fano resonances. Both are ultra-sharp resonances and could be used in highly sensitive detection of chem/bio substances (**Figure 11**).

http://dx.doi.org/10.5772/65951

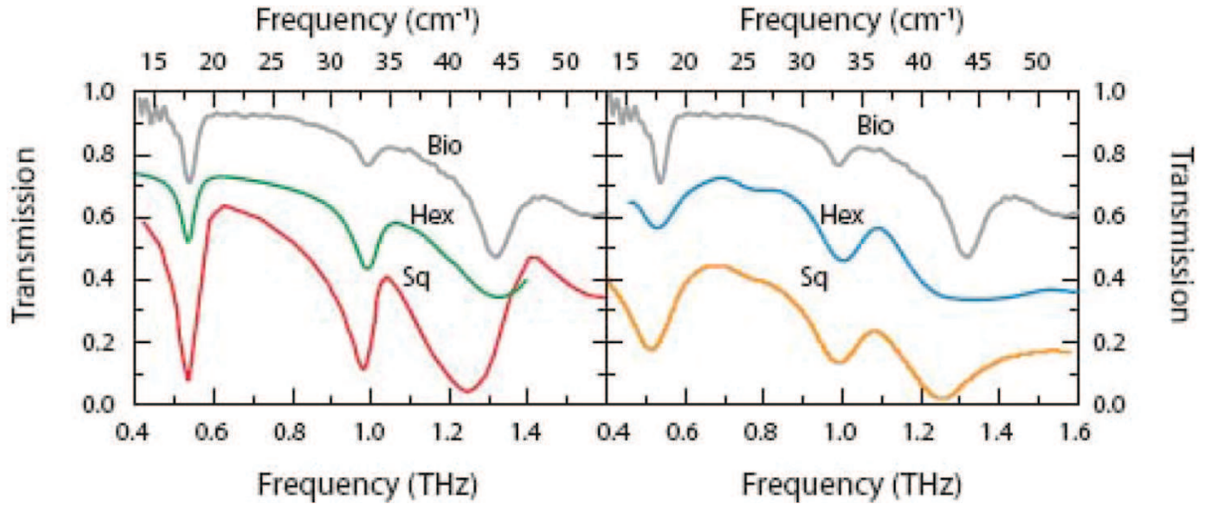

Figure 9. Computational (left) and experimental (right) measurements of the $n = 3$ hexagonal metamaterial, and the $n = 2$ square checkerboard metamaterial, compared to experimental measurements of the molecule biotin. Simulated and experimental transmission spectra of the hexagonal metamaterial has been shifted up by 20% for clarity and T(ω) of biotin is in arbitrary units [18] (Reproduced with permission of OSA).

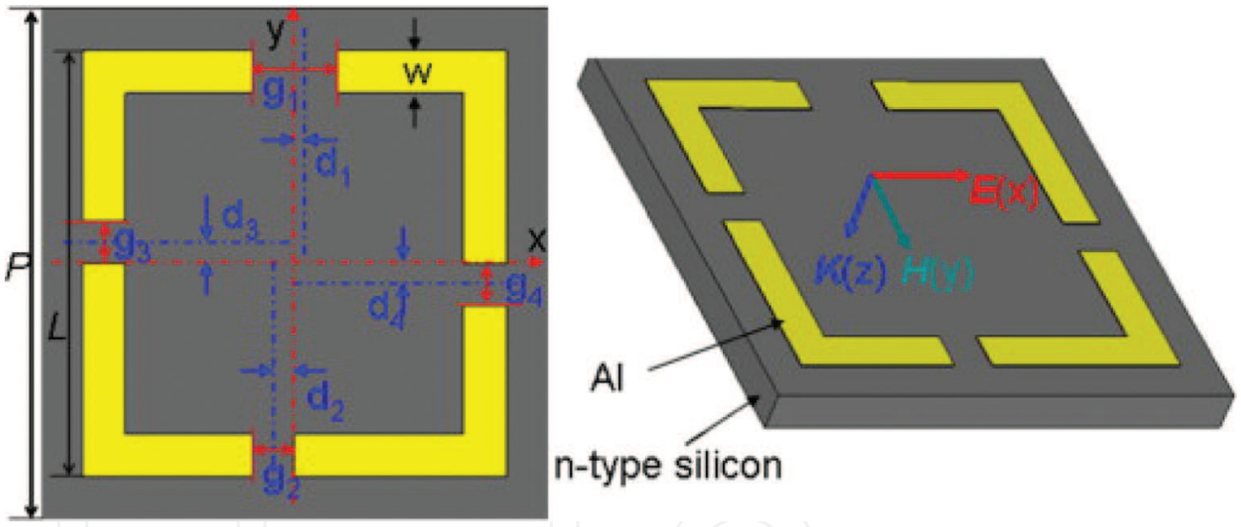

Figure 10. The front and oblique views of the unit cell of the metamaterial with asymmetrical gaps $g_1 = g_2 = g_3 \neq g_4$ [22] (Reprinted with permission from Elsevier via Copyright Clearance Center).

Again, it can be suggested that applying a layer of easily tunable complex oxide thin film can significantly enhance the agility of the proposed device since such a device would be capable of handling multiple resonant frequencies on the same surface due to the dependence of the resonance response of the device on dielectric properties of the substrate.

Metamaterial surfaces have a high potential to detect chem/bio substances in the THz spectrum. As it was mentioned before, many of these substances exhibit at least three characteristic resonant frequencies in the THz spectrum. This would make it possible to uniquely identify many materials. Unfortunately, there is no library yet compiled that can identify these unique resonant frequencies for the materials of interest.

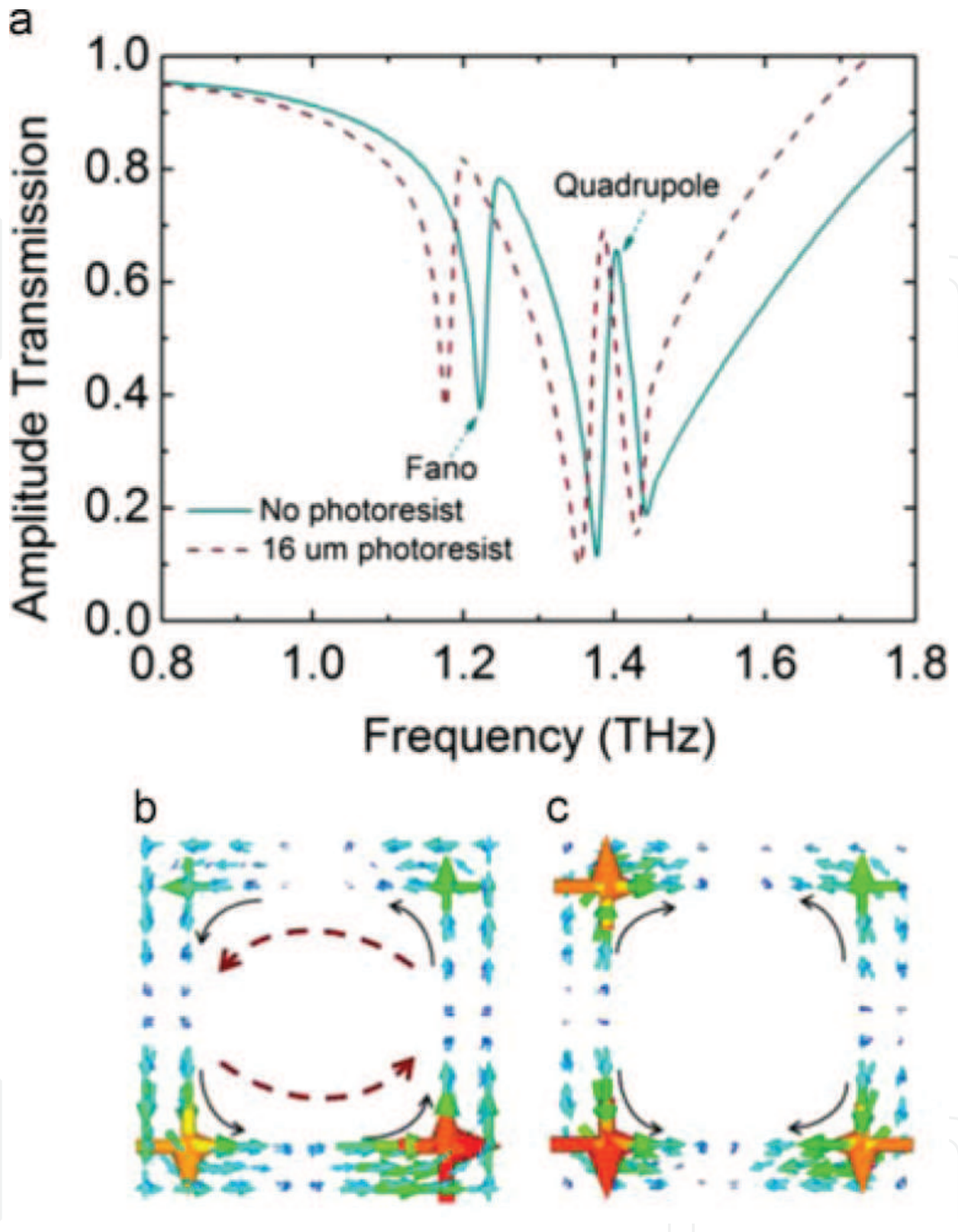

Figure 11. (a) The simulated transmission spectra of the metamaterial with (the wine line) and without (the dark cyan line) a 16 μm thick photoresist overlay. (b) and (c) The surface current distributions of the metamaterial at 1.236 and 1.408 THz, respectively [22] (Reprinted with permission from Elsevier via Copyright Clearance Center).

4. Determination of dielectric properties of complex oxide thin films in THz

Recent developments in the field of communications require higher data transmission speeds [23]. This cannot be achieved at the frequencies in which current 4G wireless systems are operating. Instead, frequencies in the range of 100 GHz are required to meet this requirement. Applications where high data transmission speeds are crucial and include holographic

http://dx.doi.org/10.5772/65951

teleconferences, improved medical sensor implants, and fast internet of things. Hence, transition to a 5G wireless system is anticipated. While optical frequencies could be a choice in terms of energy transmission in open space, this is generally not acceptable due to the eye safety concerns, power limitations, atmospheric effects, challenges in maintaining alignment between the transmitter and receiver, and, in the case of a free-space optical (FSO) communications system, the very large size of some proposed components. In a recent design, the optical front end for such a system had dimensions of 12 cm ×12 cm ×20 cm, and a weight of almost 1 kg. Therefore, low THz would be a natural choice for these applications. Indeed, Facebook © has already deployed the first experimental 5G system in a neighborhood in San Jose [24] that operates at 60 GHz. However, as an example of the difficulties associated with these frequencies, it is worthwhile to mention that the receivers for the home units are located outside the house as the low-power signal penetrate the house walls. Also, the transducers for this system were needed on each light pole in the neighborhood due to maintenance of the strength of the signal.

There are two main technical challenges that need to be overcome to make 5G widely acceptable. First, there are no sources that are capable to emit a powerful enough signal. Second, the attenuation in the air for the electromagnetic waves in the frequencies of interest is very significant [25]. Clearly, in order to overcome these issues, a lot of thought is invested in developing more powerful sources for the electromagnetic waves at low THz frequencies.

One of the obvious ways to enhance the power of a low THz source is to design and implement suitable phased array antennas. A phased array antenna consists of multiple single antennas that operate at the same frequency, but at different phases. These antennas are used in broadcasting, radars, space probes, weather research, and other applications. A suitable design would need to be compact enough to be deployed in multiple locations at relatively short distances, but large enough to contain multiple individual antennas that operate at different phases to generate a tight "focused" beam (**Figure 12**) [26].

This approach allows the beam to be condensed (as shown in **Figure 12**), maintain certain radiation pattern, and the ability to steer the beam if necessary. It was suggested [20] that thin tunable complex oxide films such as $BaSrTiO_3$ (BST) can be used in the design and fabrication of a new generation of the phased array antenna components, such as phase shifters and filters. Indeed, such films exhibit substantial tunability of their dielectric constant upon application of a simple electrical bias (**Figure 13**).

One can see from **Figure 13** that the required fields in these materials are very high, hence, thin films with the thickness of about 200 nm must be implemented to operate with the low voltages found in realistic applications.

In order to utilize these thin film components in low THz applications such as 5G, one needs to know with a very high fidelity the dielectric properties of the films in the low THz regime. Unfortunately, it is uncertain if the methods that are used to determine the dielectric properties of the tunable complex oxide thin films at lower frequencies, such as MW probes, are going to be relevant in THz range of the electromagnetic spectrum. For example, when these thin films have been investigated at low GHz, it was necessary to replace the metal-insulator-metal (MIM) structure which was used to determine the dielectric and other properties of the complex oxide thin films at lower frequencies, with a different configuration [27]. In

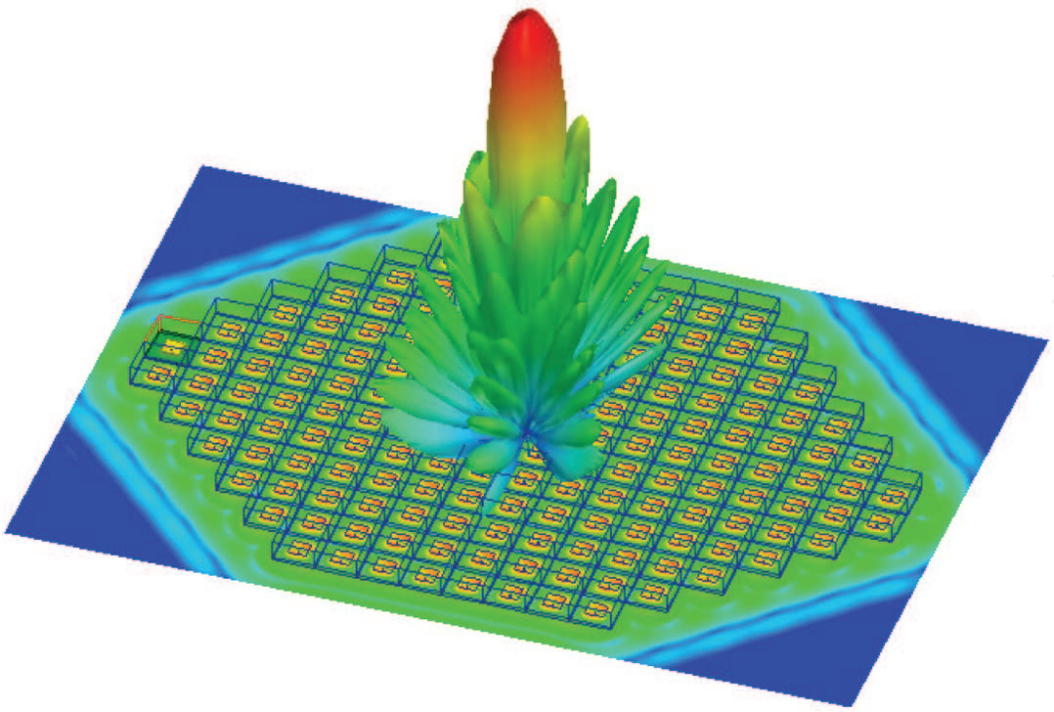

Figure 12. A model of a phased array antenna in Ansoft HFSS © commercially available software [26] (copyrighted material is reprinted with the permission of ANSYS INC©).

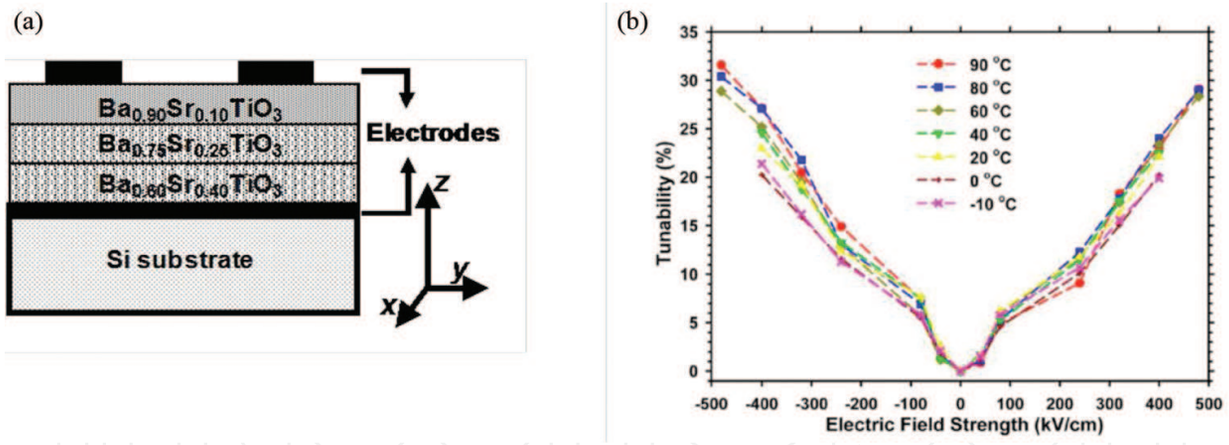

Figure 13. (a) Schematic cross section image of a BST thin film deposited on a sapphire substrate and (b) tunability plot of the BST thin film biased up to 6 V [20] (Reproduced from "Cole, M., et al., Dielectric properties of MgO-doped compositionally graded multilayer barium strontium titanate films. Appl. Phys. Lett., 2008. 92(7): p. 72906–72906", with the permission of AIP Publishing).

addition, the equipment required to perform all necessary measurements is currently very expensive. In addition, free space measurements in the THz range can help to determine the dielectric properties of thin films that are 400 nm or thicker. Therefore, a new method to measure the dielectric constant and tunability of complex oxide thin films needs to be developed. It was demonstrated in [28] that the dielectric constant of an 800 nm $BaSrTiO_3$

http://dx.doi.org/10.5772/65951

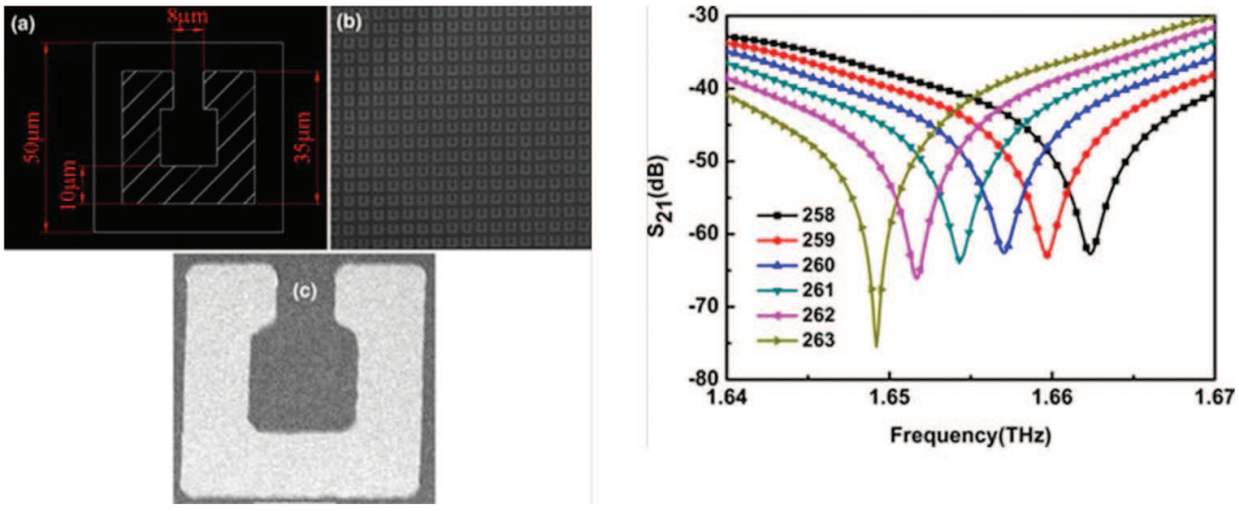

Figure 14. Schematic diagram and SEM image of a SRR unit cell with structural parameters and simulated transmission spectra of the SRRs with different dielectric constants [28] (Reproduced with permission of AMERICAN CERAMIC SOCIETY via Copyright Clearance Center).

(BST) film at low THz can be determined when a metamaterial structure is implemented on the surface of the complex oxide thin film. To do this, the resonant response of the metamaterial surface on top of the thin film is matched with a numerical model that predicts the location of this resonant peak on the frequency axis as a function of the dielectric constant of the complex oxide thin film. By matching the resonance with the numerical model, the dielectric properties (specifically, the dielectric constant) of this complex oxide thin film (**Figure 14**) can be predicted.

However, the characterization parameters that are important for the applications discussed above also include the tunability of the thin film. For the purposes of phase shifting, we need to know how much we are able to tune the dielectric properties of the complex-oxide thin films, namely, the percentage of change in the dielectric constant as a function of the applied electrical bias. A potential path to obtain this information has been demonstrated through the design and fabrication of an active metamaterial [29]. The schematics of the device are presented in **Figure 15**. One can notice that the $BaSrTiO_3$ thin film is sandwiched between two bias electrodes and, hence, "inserted" in the capacitor gap of the standing split-ring resonator (SRR) by the bottom bias electrode (**Figure 15**). The dielectric constant of the inserted BST film can be tuned by the applied bias and the resonant frequency of this single-negative metamaterial device is shifted as a function of the dielectric properties of the thin film.

Again, the model has been developed to determine the dependence of the resonant frequency of the proposed device on the dielectric properties of the $BaSrTiO_3$ thin film situated in the SRR gap. The developed model has been adjusted to match the experimental data from the fabricated sample (**Figures 16** and **17**).

From **Figure 17**, one can conclude that the frequency shift demonstrated by the fabricated metamaterial device when the $BaSrTiO_3$ thin film is biased by up to 6 V corresponds to the change of the dielectric constant of the $BaSrTiO_3$ thin film from 180 to 170. The result is based

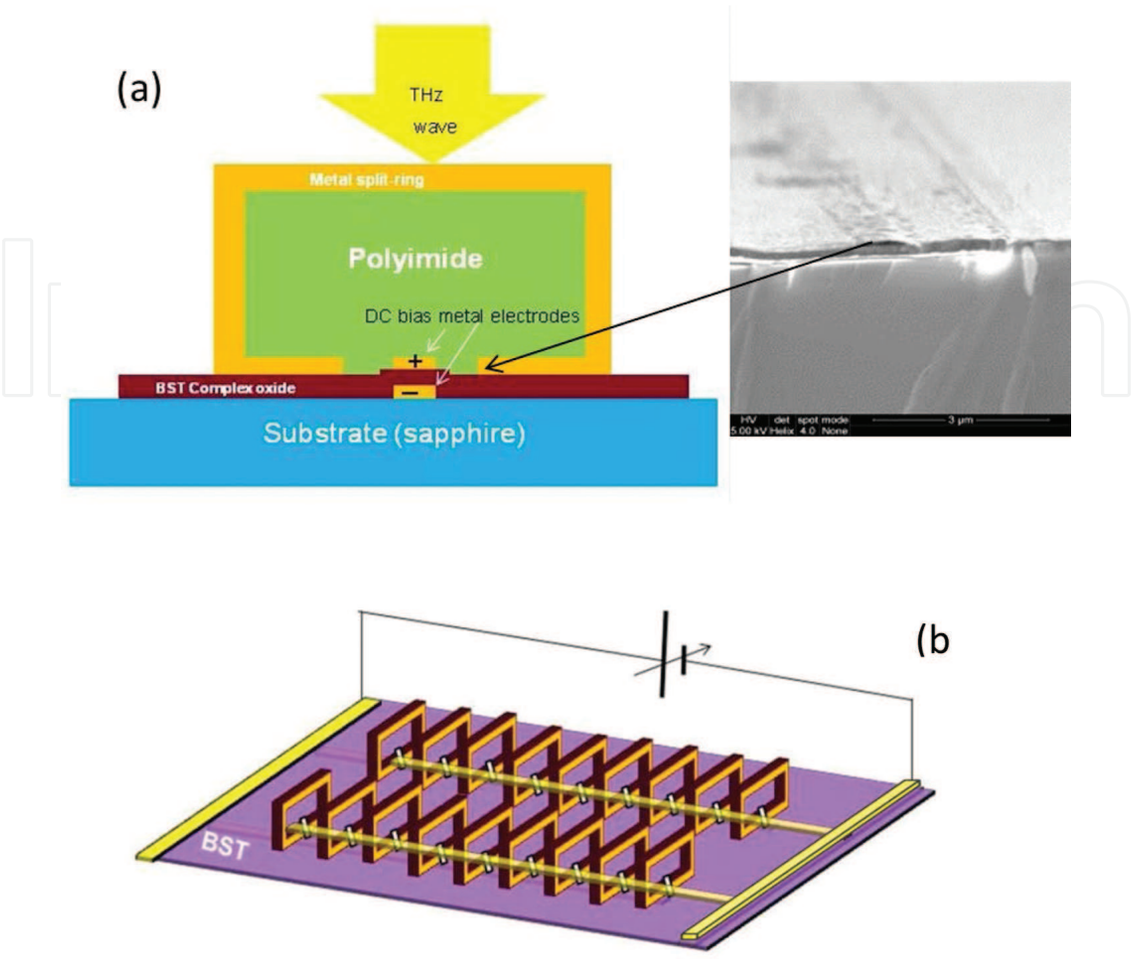

Figure 15. (a) Schematics of a tunable three-dimensional (3D) THz metamaterial unit cell with a complex oxide film as a tunable capacitor (inset: SEM image of the $BaSrTiO_3$ thin film deposited over the bias electrode). (b) 3D illustration of a complete tunable THz metamaterial device [29].

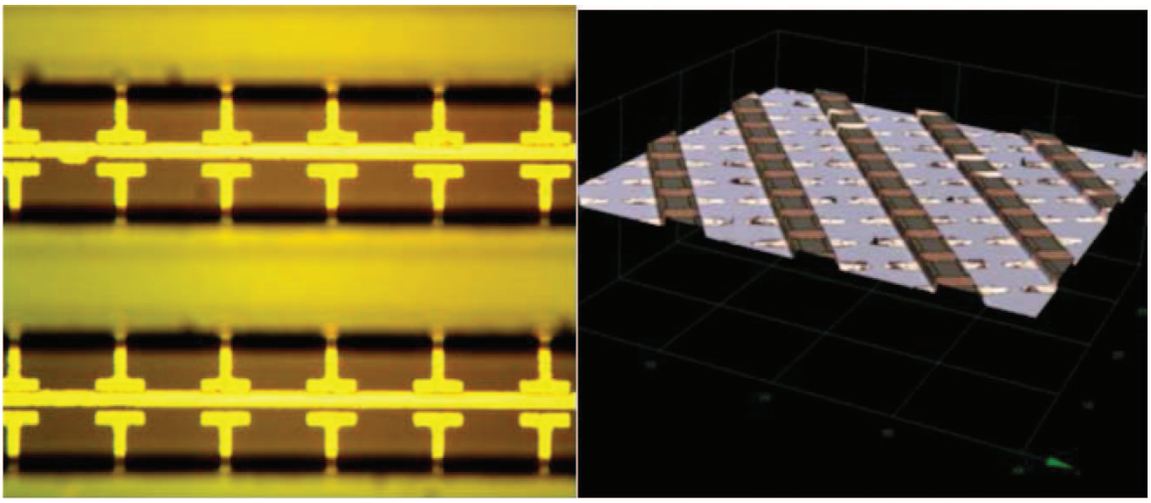

Figure 16. Left: microscopy image of the split-ring arrays focused on the bottom tunable capacitor with metal contact line; right: 3D optical microscope picture of the split-ring metamaterial device [29].

http://dx.doi.org/10.5772/65951

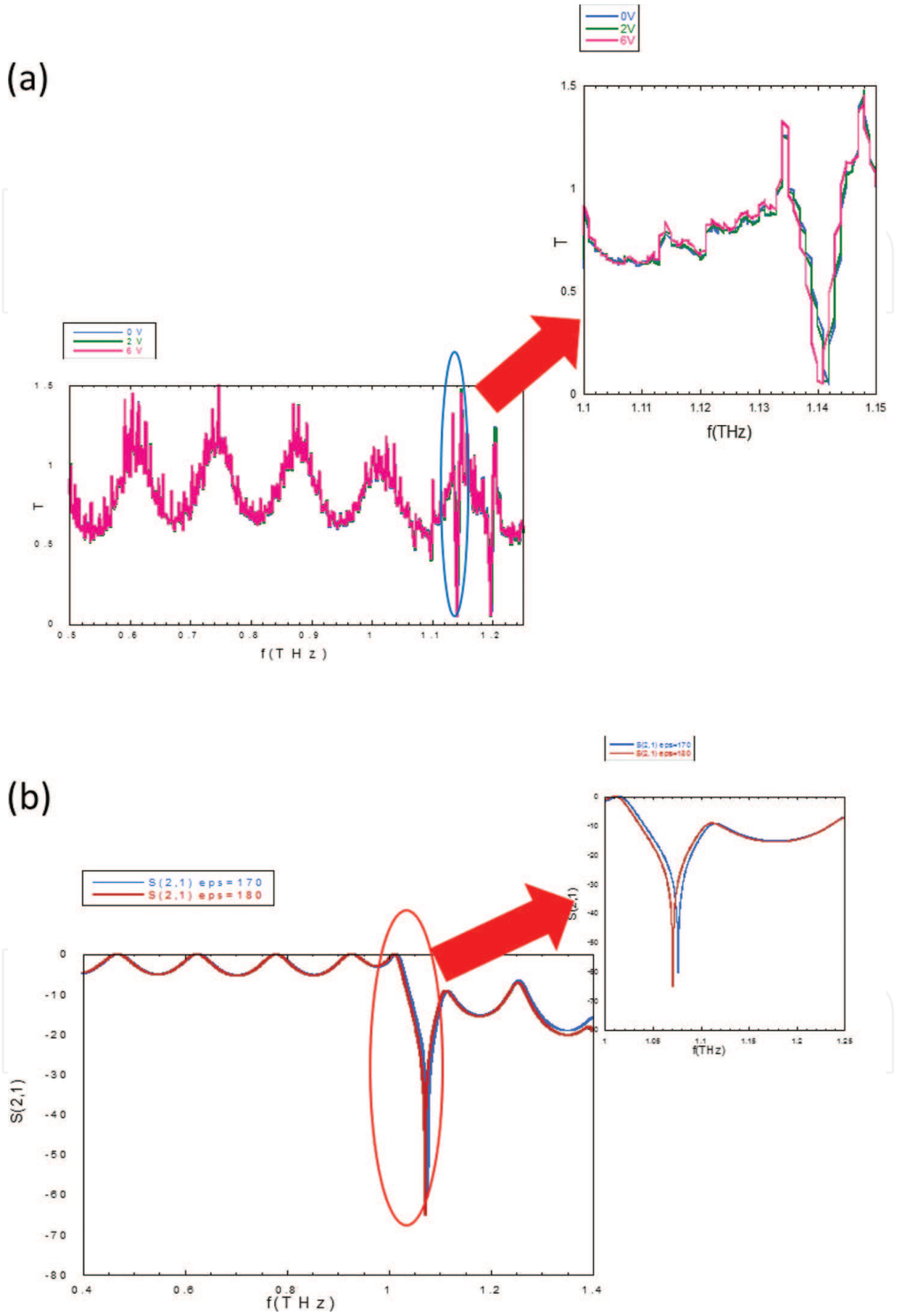

Figure 17. (a) Experimental and (b) modeled results for the metamaterial device shown in Fig. 16. A 2 GHz shift in the resonant frequency of the device is demonstrated upon application of the 6 V electrical bias [29].

on a comparison of the experimental data with the model of the single-negative metamaterial structure in HFSS© Ansoft software. This result is even more remarkable when we take into consideration the fact that in the fabricated structure (**Figure 16**), the bottom bias Pt electrode has been fabricated to the height of only 50 nm, as opposed to anticipated 200 nm to fill the gap in the metamaterial SRR completely. Hence, the fabricated metamaterial device did not operate to its utmost capacity.

The proposed approach presents an attempt to resolve an important problem of how to determine the dielectric properties of thin, tunable, complex oxide films in the THz region of radiation. Clearly, other ways to obtain this information are the source of on-going research by the scientific community. However, this approach provides a means to design devices in the frequencies of interest and serve as a standard when evaluating the fidelity of other methods, such as on-probe measurements. It was mentioned above, that alternative characterization methods exhibit certain fidelity challenges that need to be resolved in order to utilize these methods for the design and development of components operating in THz frequencies.

In addition, the presented structure constitutes an active single-negative metamaterial device. The design of the device enables reconfiguration of the structure into a double-negative metamaterial device with relative ease as opposed to other active metamaterial structures. Such a device could be used for possible THz communications or imaging applications.

5. Conclusions

This chapter attempts to expose the reader to a broader spectrum of potential metamaterial device applications, beyond antennas and geometrical optics. We have demonstrated just three potential applications that include nondestructive evaluation, chem/bio detection, and 5G communications. The intent was not to present a complete list of potential applications of metamaterial devices, as many more exist, but to give an idea of how vast the potential application space is. Metamaterials are slowly maturing from simply interesting science to becoming a very useful tool to help address multiple technical challenges in real life. Again, the presented application ideas are still at their initial point of development—either a proof-of-concept or just an idea that has been substantiated by some data. Hence, a lot of additional effort has to be invested in these areas described above to fully realize them in real-life applications. Clearly, the presented effort requires a multidisciplinary approach where fields such as electrical engineering, physics, materials science, biology, chemistry, and others are intertwined to produce a viable product.

This chapter does not attempt to present metamaterial devices as an area in which all problems have been resolved. These materials have many unresolved issues, requiring significant research investment, such as reducing transmission losses of dual-negative metamaterials. However, it is our hope that the variety of potential applications presented in this chapter will convey to the reader the extent of the impact that metamaterials can make in the future on multiple areas of technology research and development.

Acknowledgements

The author would like to thank Michael Golt of the US Army Research Lab for useful suggestions regarding the presented work.

This research was sponsored by the Army Research Laboratory and was accomplished under Cooperative Agreement Number W911NF-12-2-0019. The views and conclusions contained in this document are those of the authors and should not be interpreted as representing the official policies, either expressed or implied, of the Army Research Laboratory or the U.S. Government. The U.S. Government is authorized to reproduce and distribute reprints for Government purposes notwithstanding any copyright notation herein.

Author details

Daniel Shreiber

Address all correspondence to: daniel.shreiber.civ@mail.mil

U.S. Army Research Laboratory, Aberdeen, MD, USA

References

[1] Veselago, V., *The electrodynamics of substances with simultaneously negative values of ε and μ*. Soviet Physics Uspekhi. 1968. **10**(4): p. 509–514.

[2] Pendry, J. B., A. J. Holden, W. J. Stewart, and I. Youngs, *Extremely low frequency plasmons in metallic meso structures*. Phys. Rev. Lett, 1996. **76**: p. 4773–4776.

[3] Pendry, J. B., A. J. Holden, D. J. Robbins, and W. J. Stewart, *Magnetism from conductors and enhanced nonlinear phenomena*. IEEE Trans. Microw. Theory Tech., 1999. **47**(11): p. 2075–2084.

[4] Dong, Y and T. Itoh, *Metamaterial-based antennas*. Proc. IEEE, 2012. **100**(7): p. 2271–2285.

[5] Shelby, R. A., D. R. Smith, and S. Schultz, *Experimental verification of a negative index of refraction*. Science, 2001. **292**(5514): p. 77–79.

[6] Pendry, J. B., *Negative refraction makes a perfect lens*. Phys. Rev. Lett., 2000. **85**(18): p. 3966–3969.

[7] Ueda, T and T. Itoh, *Mu-negative, double-negative, and composite right/left handed metamaterials based on dielectric resonators*. IEICE Electron. Express, 2012. **9**(2): p. 65–80.

[8] Lai, A., T. Itoh, and C. Caloz, *Composite right/left-handed transmission line metamaterials*. IEEE Microw. Mag., 2004. **5**(3): p. 34–50.

[9] Shreiber, D., M. Gupta, and R. Cravey, *Comparative study of 1-D and 2-D metamaterial lens for microwave nondestructive evaluation of dielectric materials*. Sens. Actuators A: Phys., 2011. **165**(2): p. 256–260.

[10] Shibuya, K., K. Takano, N. Matsumoto, H. Miyazaki, K. Izumi, Y. Jimba, and M. Hangyo, "Terahertz metamaterials composed of TiO_2 cube arrays". Proceedings of the Second International Congress on Advanced Electromagnetic Materials in Microwaves and Optics - Metamaterials, Pamplona, Spain 2008.

[11] Soukoulis, C. M., S. Linden, and M. Wegener, *Negative refractive index at optical wavelengths*. Science, 2007. **315**(5808): p. 47–49.

[12] Cummer, S.A., J. Christensen, and A. Alù, *Controlling sound with acoustic metamaterials*. Nat. Rev. Mater., 2016. **1**: p. 16001.

[13] Kharkovsky, S., et al., *Dual-polarized near-field microwave reflectometer for noninvasive inspection of carbon fiber reinforced polymer-strengthened structures*. IEEE Trans. Instrum. Meas., 2008. **57**(1): p. 168–175.

[14] Tabib-Azar, M., et al., *Nondestructive superresolution imaging of defects and nonuniformities in metals, semiconductors, dielectrics, composites, and plants using evanescent microwaves*. Rev. Sci. Instrum., 1999. **70**(6): pp. 2783–2792.

[15] Shreiber, D., M. Gupta, and R. Cravey, *Microwave nondestructive evaluation of dielectric materials with a metamaterial lens*. Sens. Actuators A: Phys., 2008. **144**(1): pp. 48–55.

[16] Walther, M., et al., *Far-infrared vibrational spectra of all-trans, 9-cis and 13-cis retinal measured by THz time-domain spectroscopy.* Chem. Phys. Lett., 2000. **332**(3–4): pp. 389–395.

[17] Fischer, B., M. Walther, and P.U. Jepsen, *Far-infrared vibrational modes of DNA components studied by terahertz time-domain spectroscopy.* Phys. Med. Biol., 2002. **47**(21): p. 3807.

[18] Bingham, C. M., et al., *Planar wallpaper group metamaterials for novel terahertz applications*. Opt. Express, 2008. **16**(23): p. 18565–18575.

[19] Cole, M. W., et al., *The fabrication and material properties of compositionally multilayered* $Ba_{1-x}Sr_xTiO_3$ *thin films for realization of temperature insensitive tunable phase shifter devices*. J. Appl. Phys., 2007. **102**(3): p. 034104.

[20] Cole, M., et al., *Dielectric properties of MgO-doped compositionally graded multilayer barium strontium titanate films*. Appl. Phys. Lett., 2008. **92**(7): p. 72906–72906. http://doi.org/10.1063/1.2870079

[21] Shreiber, D., et al., *Some unusual behavior of dielectric properties of* $SrTiO_3$ *metal organic chemical vapor deposition grown thin films*. J. Appl. Phys., 2014. **116**(9): p. 094101.

[22] Ding, C. F., et al., *Dual-band ultrasensitive THz sensing utilizing high quality Fano and quadrupole resonances in metamaterials*. Opt. Commun., 2015. **350**: p. 103–107.

[23] Akyildiz, I.F., J.M. Jornet, and C. Han, *Terahertz band: next frontier for wireless communications*. Phys. Commun., 2014. **12**: p. 16–32.

[24] https://code.facebook.com/posts/1072680049445290/introducing-facebook-s-new-terrestrial-connectivity-systems-terragraph-and-project-aries/

[25] D'Amico, C., et al., *Conical forward THz emission from femtosecond-laser-beam filamentation in air*. Phys. Rev. Lett., 2007. **98**(23): 235002 p.

[26] *ANSYS web site*.

[27] Sheng, S., et al., *Characterization of microwave dielectric properties of ferroelectric parallel plate varactors*. J. Phys. D: Appl. Phys., 2009. **42**(1): p. 015501.

[28] Qi, P., et al., *Dielectric Properties of $Ba_{0.7}Sr_{0.3}TiO_3$ Film at terahertz measured by metamaterials*. J. Am. Ceram. Soc., 2012. **95**(4): p. 1167–1169.

[29] Weimin Zhou, G.D., Monica Taysing-Lara, Grace Metcalfe, Nathaniel Woodward, Amir Zaghloul, Daniel Shreiber, Melanie Cole, Eric Ngo, Matt Ivill, *Metamaterial and Metastructural Architectures for Novel C4ISR Devices and Sensors*. US Army Research Lab Tech Report, 2015.

IntechOpen